# Dichloro- bis -(pyridine-2-yl-undecyl-amine)zinc(II), [ZnCl 2 (C 16 N 2 H 26 ) 2 ]. Synthesis, characterization and antimalarial activity

**Article** *in* Journal of Coordination Chemistry · June 2016

DOI: 10.1080/00958972.2016.1204443

CITATIONS
0

READS
48

**5 authors**, including:

Hijazi Abu Ali
Birzeit University
**58** PUBLICATIONS **331** CITATIONS
SEE PROFILE

Salam Maloul
Birzeit University
**4** PUBLICATIONS **12** CITATIONS
SEE PROFILE

Mutaz Akkawi
Al-Quds University
**40** PUBLICATIONS **375** CITATIONS
SEE PROFILE

Suhair Jaber
Al-Quds University
**13** PUBLICATIONS **24** CITATIONS
SEE PROFILE

Journal of Coordination Chemistry

ISSN: 0095-8972 (Print) 1029-0389 (Online) Journal homepage: http://www.tandfonline.com/loi/gcoo20

# Dichloro-bis-(pyridine-2-yl-undecyl-amine)zinc(II), $[ZnCl_2(C_{16}N_2H_{26})_2]$: Synthesis, characterization and antimalarial activity

Hijazi Abu Ali, Salam Maloul, Issa Abu Ali, Mutaz Akkawi & Suhair Jaber

**To cite this article:** Hijazi Abu Ali, Salam Maloul, Issa Abu Ali, Mutaz Akkawi & Suhair Jaber (2016) Dichloro-bis-(pyridine-2-yl-undecyl-amine)zinc(II), $[ZnCl_2(C_{16}N_2H_{26})_2]$: Synthesis, characterization and antimalarial activity, Journal of Coordination Chemistry, 69:16, 2514-2522, DOI: 10.1080/00958972.2016.1204443

**To link to this article:** http://dx.doi.org/10.1080/00958972.2016.1204443

JOURNAL OF COORDINATION CHEMISTRY, 2016
VOL. 69, NO. 16, 2514–2522
http://dx.doi.org/10.1080/00958972.2016.1204443

Taylor & Francis
Taylor & Francis Group

# Dichloro-*bis*-(pyridine-2-yl-undecyl-amine)zinc(II), $[ZnCl_2(C_{16}N_2H_{26})_2]$: Synthesis, characterization and antimalarial activity

Hijazi Abu Ali[a,†], Salam Maloul[a,†], Issa Abu Ali[b], Mutaz Akkawi[c] and Suhair Jaber[c]

[a]Department of Chemistry, Birzeit University, West Bank, Palestine; [b]Doctor of Pharmacy Program, Birzeit University, West Bank, Palestine; [c]Department of Life Sciences, Al-Quds University, West Bank, Palestine



**ABSTRACT**

A nitrogen-based ligand (pyridine-2-yl-undecyl-amine) (**1**) was synthesized and used for the synthesis of a Zn(II) compound (dichloro-bis(pyridine-2-yl-undecyl-amine)zinc(II)) (**2**). Compound **2** was synthesized and characterized using IR, $^1$H NMR, and $^{13}$C{$^1$H} NMR spectroscopy. The crystal structure of **2** was determined using single-crystal X-ray crystallography. The compound was tested for its anti-malarial activity using two methods, a semi-quantitative micro-assay and a previously self-developed quantitative *in vitro* method. Both methods were used to study the efficiency of **2** to inhibit the formation of the malaria pigment considered an important target of many anti-malarial drugs such as chloroquine and amodaquine. The efficiency of **2** to prevent the formation of β-hematin was 71.4%. The efficiency of amodiaquine as a standard drug was reported at 93.8%.

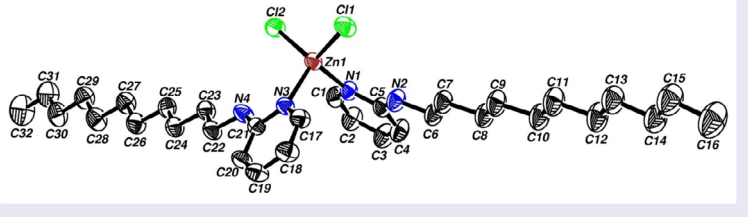


**ARTICLE HISTORY**
Received 29 January 2016
Accepted 3 May 2016

**KEYWORDS**
Malaria; zinc complexes; nitrogen-based ligands; β-hematin

## 1. Introduction

Zinc plays a very important role in the living body [1]. Zinc occurs naturally as the divalent cation $Zn^{2+}$ and has no redox activity under physiological conditions. Zn(II) is a strong intracellular Lewis acid, coordinating to proteins via either the cysteine residues or the amino ligands of histidine residues or sulfur "thiol" moieties [2].

Many nitrogen-based ligands have been synthesized and their biological activity studied [3–9]. Studies have shown that heterocyclic nitrogen plays an important role in coordination chemistry. Heterocycles which contain more than one nitrogen are key structures in a large variety of biochemical processes. These ligands exhibit various coordination modes in metal complexes [10, 11].

**CONTACT** Hijazi Abu Ali habuali@birzeit.edu
Supplemental data for this article can be accessed at http://dx.doi.org/10.1080/00958972.2016.1204443.
[†]These authors contributed equally to this work.

Different studies have shown that the interaction of metal ions with bioactive organic compounds increases the biological activity of the ligands [3, 12]. Many factors determine the relationship between the structure and activity of the compounds. Among these factors are the metal oxidation state, the type and number of donors, as well as their relative position within the ligands [3, 13].

Malaria is a prevalent parasitic disease. As reported by the World Health Organization and according to the World Malaria Report of 2015 [14], Africa is the most affected continent with about 91% of all malarial deaths [15]. Plasmodium, the parasite causing malaria, is the single most devastating protozoan [16]. There are five species of plasmodium that may cause human malaria, but *plasmodium falciparum* is the most fatal species [17].

The parasite lives within human red blood cells and consumes over two-thirds of the hemoglobin of the host cell [18]. During its intraerythrocytic stage, the parasite degrades hemoglobin for its biosynthetic requirements. Large amounts of free heme known as ferriprotoporphyrin (IX) are released [17]. The accumulation of ferriprotoporphyrin (IX) causes the generation of reactive oxygen species which may induce oxidative stress leading to parasitic death [15]. The parasite avoids these toxic effects by polymerizing these heme molecules within the food vacuole at pH 4.5–5.0, into a nontoxic, unreactive, insoluble crystalline compound called hemozoin or "malaria pigment" [17]. Hemozoin formed in this unique life cycle is an important target in the search of new antimalarial drugs [19, 20]. A synthetic analog to hemozoin called β-hematin is structurally and spectroscopically identical to purified hemozoin [19], making it an excellent target for biochemistry studies [21]. Structurally, hemozoin consists of reciprocal head-to-tail dimeric units of heme bound through propionate oxygen-iron(III) [19, 21]. The propionic acid groups of the heme dimer are then hydrogen bonded with other dimers to form extended crystals. Since it is a process that is essential to the survival of the malaria parasite, it acts as an excellent target for *in vitro* study. Drugs are thought to act by inhibiting the formation of hemozoin in the food vacuole of the parasite. This prevents detoxification of the free heme released in this compartment, killing thus the parasite [19, 21].

Ring-used heterocycles which contain more than one nitrogen are key structures in a large variety of biochemical processes [10]. Compounds may coordinate through the exocyclic amino group attached directly to the ring or more probably through nitrogen of the endocyclic ring. Either way the mechanism of inhibition is thought to be through complexation which prevents the formation of β-hematin. Chloroquine, a quinoline-ring drug, is widely used for malaria treatment, and it inhibits heme polymerization "β-hematin formation" through complex formation with ferriheme monomers [22].

However, resistance to chloroquine has increased, owing to extensive and uncontrolled use. Chloroquine resistance and toxicity are considered as major challenges, and the need for new effective antimalarial drugs exists [23]. In this study, we describe the structure and the antimalarial activity of a new zinc chloride with nitrogen-based ligand. The ligand contains both hydrophilic and hydrophobic groups, which play a crucial role in its structure activity relationship. The crystal structure, spectroscopic properties, and antimalarial potential of **2** are reported.



## 2. Results and discussion

### 2.1. Synthesis

Compound **1** was prepared by reacting 1 eq of undecane bromide with 1 eq of 2-aminopyridine in THF. The desired product was obtained as a yellow precipitate. Compound **2** was synthesized by mixing **1** with $ZnCl_2$ in THF; the residues were crystallized to give a white precipitate (scheme 1).

### 2.2. X-ray crystallographic study of [$ZnCl_2$(pyridine-2-yl-undecyl-amine)$_2$]

The geometry for **2** has been confirmed by single-crystal X-ray crystallography. Figure 1 shows an ORTEP view of the molecule and Table S1 and Table 1 summarize atomic parameters and significant bond

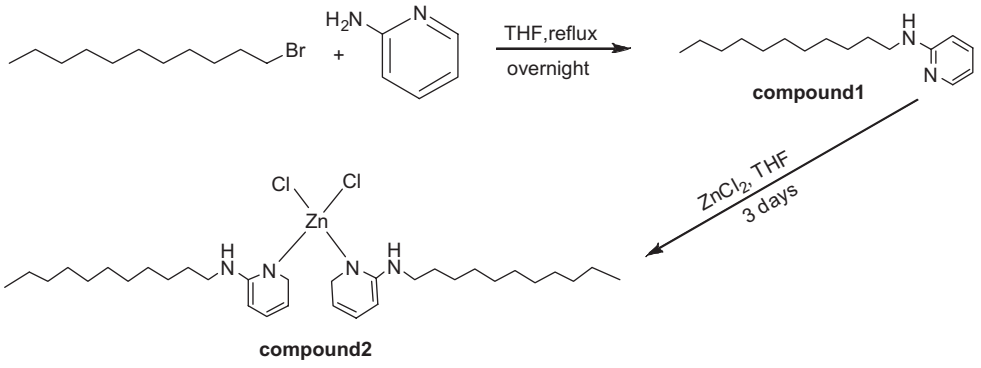


**Scheme 1.** Synthesis of **1** and **2**.

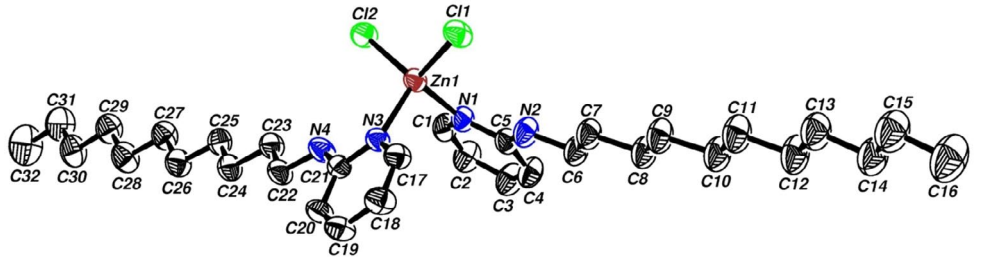


**Figure 1.** View of the molecular structure of **2** showing the atom labeling scheme.

**Table 1.** Selected bond distances (Å) and angles (°) for **2**.

| Bond distances | (Å) | Bond angles | (°) |
|---|---|---|---|
| Cl(1)–Zn(1) | 2.2271(5) | N(3)–Zn(1)–N(1) | 100.65(6) |
| Cl(2)–Zn(1) | 2.2367(5) | Cl(1)–Zn(1)–Cl(2) | 114.20(2) |
| N(1)–Zn(1) | 2.0612(17) | C(1)–N(1)–Zn(1) | 115.71(13) |
| N(3)–Zn(1) | 2.0504(15) | C(5)–N(1)–Zn(1) | 125.63(13) |
| C(21)–N(4) | 1.353(3) | N(2)–C(5)–N(1) | 117.63(19) |
| C(21)–N(3) | 1.354(2) | N(4)–C(21)–N(3) | 117.52(17) |
| C(22)–N(4) | 1.452(2) | C(21)–N(4)–C(22) | 123.59(18) |

lengths and angles, respectively. The zinc is four-coordinate generating a distorted tetrahedral coordination environment. Two coordination sites are occupied by the N-donors of **1** while the remaining coordination sites are occupied by chlorides. However, the bond angle N(3)-Zn(1)–N(1) of 100.65(6)° is low for a typical tetrahedral geometry, resulting in a distortion [24, 25].

The two Zn–Cl distances Cl(1)–Zn(1) (2.2271(5) Å) and Cl(2)–Zn(1) (2.2367(5) Å), due to symmetry reasons, are approximately equal in length; they are similar to previously reported values [3, 24–28]. Compound **2** exhibits Zn–N bonds of the same length with values 2.0612(17) and 2.0504(15) Å.

Table S2 shows two intramolecular hydrogen bonds between N(2) and C1(1), N(4) and Cl(2) with distances of 3.331(2) and 3.3014(19) Å, respectively. These values are comparable with previously reported values in similar complexes [27]. This identical hydrogen bonding also supports the fact that the bond distances of Cl(1)–Zn(1) and Cl(2)–Zn(1) are similar, while in reported complexes there was lengthening of the Zn–Cl(1) bond related to the presence of an intramolecular hydrogen bond, since Cl(2) does not form such a bond [29].

### 2.3. Infrared and UV–vis spectra

The infrared (IR) frequencies from 4000 to 190 $cm^{-1}$ and UV–vis bands for 2-aminopyridine in **1** and **2** are given in Table S3. The Zn–Cl and Zn–N stretching frequencies are at 300, 321 $cm^{-1}$ and 205, 245 $cm^{-1}$, respectively, and were assigned by comparison with those reported for similar complexes [30, 31]. As expected, the two peaks for *v*N–H in 2-aminopyridine (3330, 3205 m) were observed as one peak in **1** and **2** and shifted to lower energy, confirming the formation of **1** and **2**. This shift to lower energy may be due to hydrogen bond formation between the N–H hydrogen and chloride as supported by the crystal structure of **2** [30, 31].

The absorption spectrum of **2** in DMSO is very similar to that of the parent N-donor ligand with only 1-nm shift caused by coordination to zinc. Thus, all bands of **2** are based to ligand. The spectra are also similar to zinc complexes of N-donor ligands [3, 26, 28].

### 2.4. $^{1}H$ NMR and $^{13}C\{^{1}H\}$ NMR results

$^{1}H$ NMR and $^{13}C\{^{1}H\}$ NMR data and parameters of **2** and its parent ligand are listed in the section 4. For **2**, the NMR resonances and chemical shifts are supported by the X-ray structure. The N**H** resonance at 4.53 ppm is up-field shifted to 7.16 ppm in **2** due to complexation and hydrogen bonding with $Cl^{-}$. The C$\mathbf{H}_2$NH resonance at 3.23 ppm is down-field shifted to 3.14 ppm in **2**. The pyridine ring hydrogen resonances are almost identical in **2** and its parent ligand. The $^{13}C\{^{1}H\}$ NMR chemical shifts for **2** and its parent ligand are similar. However, the resonance for **C**$H_2$NH at 42.30 ppm in the ligand was down-field shifted to 43.01 ppm in **2**.

### 2.5. Antimalarial activity

Before measurement of its antimalarial activity, the solution stability of **2** was checked by recording periodically the $^{1}H$ and $^{13}C$ NMR spectra in chloroform and DMSO which always gave the same data. In addition, **2** was crystallized by slow solvent evaporation at room temperature that took several days, and the NMR measurements were repeated to give the same physical properties of the compound.

A semi-quantitative *in vitro* method developed by Deharo *et al.* was used in this study [32]. In this microassay, the inhibitory effect of different compounds on the biomineralization of ferriprotoporphyrin IX to hemozoin or β-hematin was studied. It is based on the detection by optical density measurement of solubilized β-hematin remaining after contact with drugs. Positive controls such as chloroquine or amodiaquine will inhibit the formation of β-hematin and will give low absorbance values.

#### 2.5.1. Semi-quantitative method

Compound **2** was evaluated for its inhibitory effect on *in vitro* β-hematin formation. Results of the semi-quantitative method are shown in Figure 2. The efficiency of the drug used is inversely proportional to the absorption, since low absorption indicates higher efficiency. It is important to mention that each result is the average of 24 individual experiments. As shown in Figure 2, **2** with an absorbance value of 0.157 (at a concentration of 1 mg $mL^{-1}$) has a potential antimalarial activity when compared to the standard drugs, while no inhibition was noticed at 0.6 mg $mL^{-1}$. This result is in accord with similar previously reported zinc complexes [26, 28].

#### 2.5.2. Quantitative method

According to the method used, comparison of **2** with DMSO (as negative control) and amodiaquine (AQ as positive control) in terms of β-hematin formation is shown in Figure 3. A comparison in terms of

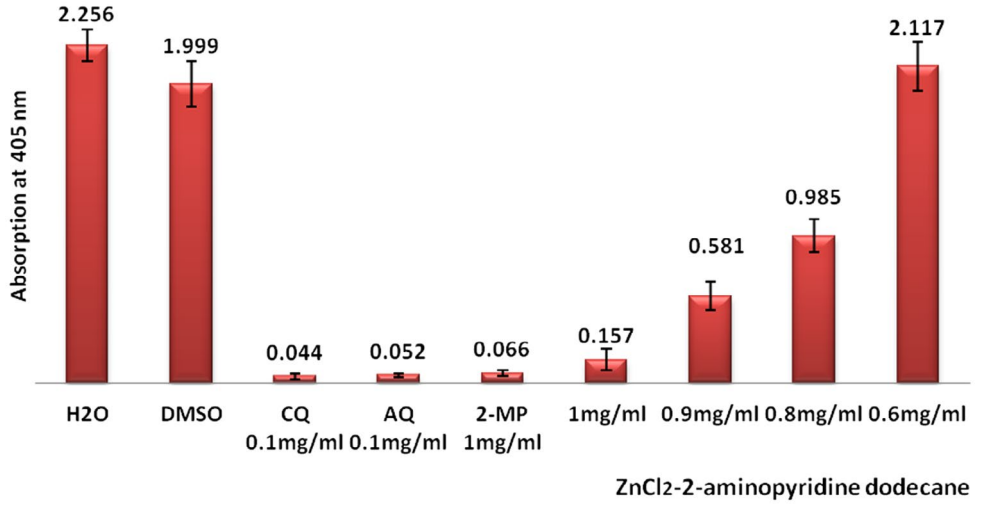


**Figure 2.** Column diagram representing semi-quantitative test results of potential antimalarial drug [$ZnCl_2$(2-aminopyridine-dodecane)$_2$] (**2**) compared to chloroquine (CQ), amodiaquine (AQ) (0.1 mg $mL^{-1}$), and 2-mercaptopyrimidine (1 mg $mL^{-1}$) as positive controls, while water and DMSO were used as negative controls. Absorption is inversely proportional to drug efficiency; the lower absorption drug is considered to be more efficient. Results are the average of 24 tests.

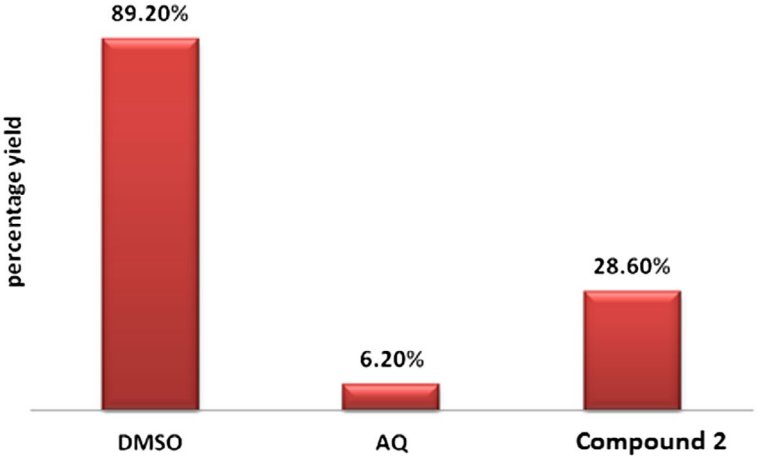


**Figure 3.** Column diagram representing the percentage yield of **2** compared to amodiaquine and DMSO at 0.4 mM. Yields are inversely proportional to drug efficiency; the lower yield drug is considered to be more efficient.

drug efficiency is shown in Figure 4. Figure 3 represents the percentage yield of β-hematin formation. Interestingly, the percentage yield of β-hematin formation in the presence of **2** was 28.6% and that of AQ was 6.2%, both at 0.4 mM concentration comparing to the negative control which was 89.2%. A comparison in terms of efficiency of **2** is shown in Figure 4. It is obvious that **2** has antimalarial activity in inhibiting β-hematin formation with efficiency of 71.4% when compared to AQ (93.8%) and DMSO (10.8%).

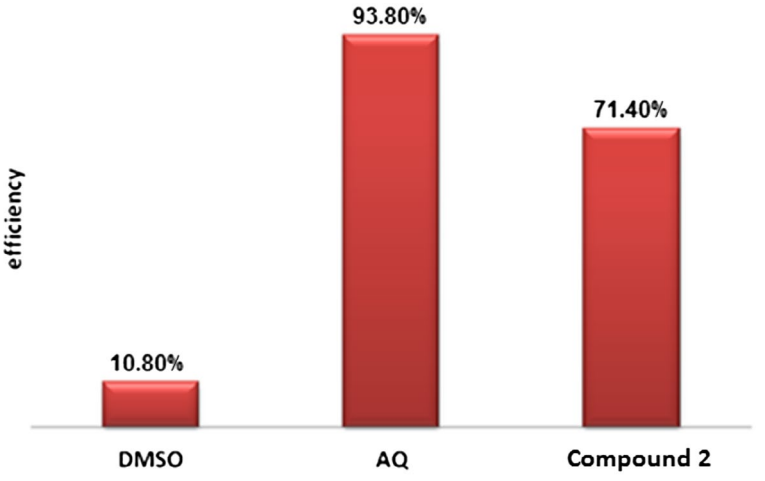


**Figure 4.** Column diagram representing the efficiency of **2** compared to amodiaquine and DMSO, all at a concentration of 0.4 mM.



## 3. Conclusion

Compound **2** and its parent ligand were synthesized and characterized by various spectrometric techniques including X-ray crystallography, $^{1}$H NMR, $^{13}$C{$^{1}$H} NMR, IR, and UV–vis. Compound **2** showed inhibition activity on the formation of β-hematin. Ongoing research will be carried out in our laboratory to study the toxicity and the *in vivo* effects of this compound to gain further understanding of their biological action. The efficiency of **2** in preventing the formation of β-hematin was 71.4% compared to 93.8% of the standard drug amodiaquine. Compound **1** did not show any inhibition activity against β-hematin formation.

## 4. Experimental

### 4.1. Instruments

Infrared absorption spectra were recorded using a Varian 600 FT-IR spectrometer from 400 to 4000 cm$^{-1}$ using KBr pellets. $^{1}$H and $^{13}$C{$^{1}$H} NMR spectra were recorded in $CDCl_3$ and DMSO ($d_6$) as solvents with a Varian Unity spectrometer (300 and 75 Hz) for $^{1}$H and $^{13}$C{$^{1}$H} nuclei, respectively. UV–vis spectra were recorded using a Hewlett Packard 8453 photo-diode array spectrophotometer from 200 to 4000 nm using DMSO as solvent. Melting points were determined in capillary tubes with EZ-melt apparatus and are uncorrected.

### 4.2. Materials

The starting materials used in the present work were purchased from Sigma-Aldrich with high purity and used without purification. Solvents were also purchased from commercial sources.

### 4.3. Synthesis

#### 4.3.1. Synthesis of pyridine-2-yl-undecyl-amine (1)

Undecane bromide (11.75 g, 0.0499 mol) dissolved in 20 ml THF was carefully added to a stirred 2-aminopyridine solution (4.72 g, 0.05 mol) dissolved in 70 ml THF. The reaction mixture was heated under reflux overnight, and then the product was extracted using 2 M NaOH and ethyl acetate. The organic

layer was dried over anhydrous magnesium sulfate and solvent was removed under vacuum. The product was purified by silica gel column chromatography with 5% ethyl acetate/petroleum ether as eluent to give the product as yellow solid.

**$C_{16}N_2H_{28}$ (1)**: 70% yield, m.p. 51 °C; $^1$H NMR ($CDCl_3$, $\delta$ (ppm)): 0.88 (t, 3H, $CH_3$, $^3J_{H-H}$ = 6.9 Hz), 1.26 (s, 16H, $CH_2$), 1.59 (p, 2H, $CH_2$, $^3J_{H-H}$ = 6.9 Hz), 3.23 (q, 2H, $CH_2$, $^3J_{H-H}$ = 6.0 Hz), 4.53 (s, 1H, NH), 6.36 (d, 1H, CH, $^3J_{H-H}$ = 8.1 Hz), 6.53 (t, 1H, CH, $^3J_{H-H}$ = 6.0 Hz), 7.40 (t, 1H, CH, $^3J_{H-H}$ = 7.5 Hz), 8.06 (d, 1H, CH, $^3J_{H-H}$ = 4.5 Hz), $^{13}$C{$^1$H} NMR ($CDCl_3$, $\delta$ (ppm)): 14.11 ($CH_3$), 22.69 ($CH_2$), 27.07 ($CH_2$), 29.33 ($CH_2$), 29.41 ($CH_2$), 29.55 ($CH_2$), 29.61 ($CH_2$), 31.91 ($CH_2$), 42.30 ($CH_2$), 106.50 (Ar, CH), 112.55 (Ar, CH), 137.41(Ar, CH), 148.67 (Ar, CH), 158.50 (Ar, C); IR (cm$^{-1}$, KBr): 3268 (m, $\nu$(N–H)), 2923 (s, $\nu$(C–H)$_{aromatic}$), 2851 (s, $\nu$(C–H)$_{aliphatic}$), 1604 (s, $\nu$(C=C)$_{ring}$), 1528 (s, $\nu$(C=C)$_{ring}$), 802 (m, $\gamma$(C–H)$_{aromatic}$). UV–vis, (DMSO, $\lambda$ (nm)): 259, 275.

#### 4.3.2. Synthesis of [$ZnCl_2$(pyridine-2-yl-undecyl-amine)$_2$] (2)

Pyridine-2-yl-undecyl-amine (0.496 g, 0.002 mol) dissolved in 20 mL THF was added to a stirred $ZnCl_2$ solution (0.272 g, 0.002 mol) dissolved in 30 mL THF. The reaction mixture was stirred at room temperature for 3 days; then, the residue was washed with ethyl acetate, air-dried, and recrystallized from hot acetone to give colorless crystals.

**[$ZnCl_2(C_{16}N_2H_{26})_2$] (2)**: 50% yield, m.p. 98 °C; $^1$H NMR ($CDCl_3$, $\delta$ (ppm)): 0.88 (t, 3H ,$CH_3$, $^3J_{H-H}$ = 6.6 Hz), 1.25 (s, 16H, $CH_2$), 1.40 (t, 2H, $CH_2$, $^3J_{H-H}$ = 7.5 Hz), 1.68 (p, 2H, $CH_2$, $^3J_{H-H}$ = 7.2 Hz), 3.14 (q, 2H, $CH_2$, $^3J_{H-H}$ = 3.9 Hz), 6.55 (d, 1H, CH, $^3J_{H-H}$ = 8.1 Hz), 6.61 (t, 1H, CH, $^3J_{H-H}$ = 5.7 Hz), 7.16 (s, 1H, NH), 7.61 (t, 1H, CH, $^3J_{H-H}$ = 7.5 Hz), 8.05 (d, 1H, CH, $^3J_{H-H}$ = 4.5 Hz); $^{13}$C{$^1$H} NMR ($CDCl_3$, $\delta$ (ppm)): 14.12 ($CH_3$), 22.68 ($CH_2$), 26.97 ($CH_2$), 28.55 ($CH_2$), 29.29 ($CH_2$), 29.33 ($CH_2$), 29.53 ($CH_2$), 29.61 ($CH_2$), 31.90 ($CH_2$), 43.01($CH_2$), 107.61 (Ar, CH), 112.29 (Ar, CH), 124.23(Ar, CH), 146.32 (Ar, CH), 158.50 (Ar, C); IR (cm$^{-1}$, KBr): 3301 (s, $\nu$(N–H)), 2922 (s, $\nu$(C–H)$_{aromatic}$), 2849 (s, $\nu$(C–H)$_{aliphatic}$), 1617 (s, $\nu$(C=C)$_{ring}$), 1574 (s, $\nu$(C=C)$_{ring}$), 773 (m, $\gamma$(C–H)$_{aromatic}$), 245 (m, $\nu$(Zn–N)), 321 (m, $\nu$(Zn–Cl)). UV–vis (DMSO, $\lambda$ (nm)): 259, 276.

### 4.4. X-ray crystallography

X-ray intensity data of **2** were obtained at room temperature on a Bruker SMART APEX CCD X-ray diffractometer system (graphite-monochromated Mo Kα radiation $\lambda$ = 0.71073 Å) using the SMART software package [33]. The data were reduced and integrated by SAINT [34]. The structure was solved and refined by the SHELXTL software package [35]. Hydrogens were located geometrically and treated with a riding model. Crystal data and details of the data collection and refinement are summarized in Table S1.

### 4.5. Antimalarial activity

#### 4.5.1. In vitro testing for antimalarial activity using a semi-quantitative method

The procedure for *in vitro* testing was carried out according to Deharo *et al.* [32]. A mixture containing 50 mL of (0.5 mg mL$^{-1}$) hemin chloride freshly dissolved in DMSO, 100 mL of (0.5 M) sodium acetate buffer (pH 4.4), and 50 mL of different concentrations of the compound dissolved in pure water was incubated in a normal nonsterile 96-well flat bottom plate at 37 °C for 18–24 h. It is important that the solutions be added to the plate in this order. The plate was then centrifuged for 10 min at 4000 rpm. The supernatant was removed and the pH of reaction was measured. The final pH of the mixture should be between 5.0 and 5.2. The wells were washed with 200 mL DMSO per well to remove free hemin chloride. The plate was centrifuged again, discarding the supernatant afterward. The residual β-hematin was then dissolved in 200 mL of 0.1 M NaOH to form ferriprotoporphyrin (IX) that can be measured spectrophotometrically. Finally, the absorbance was measured at 405 nm using the ELISA reader. The results acquired were compared to negative ultrapure $H_2O$ and positive chloroquine (CQ) of 0.1 mg mL$^{-1}$ and 2-mercaptopyrimidine (2-MP) of 1 mg mL$^{-1}$ controls. 2-MP is considered as an internal control to ensure that the reaction environment was ideal, that is, due to its sensitivity to the change in temperature. The absorption is inversely proportional to drug efficiency meaning the lower the absorption, the more efficient the drug.

### 4.5.2. Quantitative test

The method of Blauer and Akkawi was adopted for quantitative test [36]. Freshly prepared stock solution of hemin chloride was prepared by dissolving the salt in DMSO and incubating for 30 min at 30 °C; stock solution of the compound used was prepared using DMSO (0.5 M). Sodium acetate buffer (pH 4.4) was also prepared; the final concentration of hemin and the compound in the reaction were 0.2 and 0.4 mM, respectively. The whole mixture was left for 18–24 h at 37 °C without stirring. The total volume of the reaction mixture was 32 mL, and the final pH was 4.9–5.2. Samples were centrifuged for 10 min using a serological (Jouan B4) centrifuge. The supernatant was discarded and the precipitate was washed with DMSO and quantitatively transferred to a Millipore Swinnex 13 filter containing Whatman filter paper No. 50, already lyophilized to a constant weight in a freeze-drying machine (Labconco Freezone). DMSO was passed slowly through the filter until the filtrate remained feebly colored and washed again with ultra-pure water. The remaining solid was then lyophilized to a constant weight.

## Supplementary material

CCDC 1420242 (**2**) contains the supplementary crystallographic data for this paper. These data can be obtained free of charge from the Cambridge Crystallographic Data Center via www.ccdc.cam.ac.uk/data_request/cif.



## Acknowledgements

The authors thank the office of Vice President for Academic Affairs at Birzeit University for their financial support.

## Disclosure statement

No potential conflict of interest was reported by the authors.

## References

[1] J. Yao, Y. Liu, H.G. Liang, C. Zhang, J.Z. Zhu, X. Qin, M. Sun, S.S. Qu, Z.N. Yu. *J. Therm. Anal. Calorim.*, **79**, 39 (2005).
[2] D.K. Blencowe, A.P. Morby. *FEMS Microbiol. Rev.*, **27**, 291 (2003).
[3] (a) H. Abu Ali, M.D. Darawsheh, E. Rappocciolo. *Polyhedron*, **61**, 235 (2013); (b) H. Abu Ali, B. Jabali. *Polyhedron*, **107**, 97 (2016); (c) H. Abu Ali, S. Omar, M. Darawsheh, H. Fares. *J. Coord. Chem.*, **69**, 1110 (2016).
[4] H. Chiririwa, E. Muzenda. *Proc. World Congr. Eng. Comput. Sci.*, **II**, 22 (2014).
[5] I. Ali, W.A. Wani, K. Saleem, A. Haque. *Curr. Drug Ther.*, **7**, 13 (2012).
[6] I. Ali, A. Haque, K. Saleem, M.F. Hsieh. *Bioorg. Med. Chem.*, **21**, 3808 (2013).
[7] I. Ali, K. Saleem, D. Wesselinova, A. Haque. *Med. Chem. Res.*, **22**, 1386 (2012).
[8] I. Ali, W.A. Wani, A. Khan, A. Haque, A. Ahmad, K. Saleem, N. Manzoor. *Microb. Pathog.*, **53**, 66 (2012).
[9] K. Saleem, W.A. Wani, A. Haque, M.N. Lone, M.-F. Hsieh, M.A. Jairajpuri, I. Ali. *Future Med. Chem.*, **5**, 135 (2013).
[10] B. Ashish, S.N. Pandeya. *Int. J. Res. Ayureveda Pharm.*, **2**, 1124 (2011).
[11] I. Ali, M. Lone, Z. Al-Othman, A. Al-Warthan, M. Sanagi. *Curr. Drug Targets*, **16**, 711 (2015).
[12] Y.-Y. Yu, H.-D. Xian, J.-F. Liu, G.-L. Zhao. *Molecules*, **14**, 1747 (2009).
[13] S. Atmaca. *Tr. J. Med. Sci.*, **28**, 595 (1998).
[14] W.H. Organization. *World Health Stat.*, 2015 (2015).
[15] S. Kumar, M. Guha, V. Choubey, P. Maity, U. Bandyopadhyay. *Life Sci.*, **80**, 813 (2007).
[16] L.H. Bannister, I.W. Sherman. *Encyclopedia of Life Sciences*, John Wiley & Sons, Ltd., Chichester (2009).
[17] R. D. Strategies for Malaria Control VBI Scientific Annual Report, pp. 49–53 (2006).
[18] B. Sekhon, N. Bimal. *J. Pharm. Educ. Res.*, **3**, 52 (2012).
[19] A.F. Slater, W.J. Swiggard, B.R. Orton, W.D. Flitter, D.E. Goldberg, A. Cerami, G.B. Henderson. *Proc. Natl. Acad. Sci. USA.*, **88**, 325 (1991).
[20] D.J. Sullivan. In *Biopolymers*, S. Matsumura, A. Steinbüchel (Eds.), Online, pp. 129–137, Wiley-VCH Verlag GmbH & Co. KGaA, Weinheim, Germany (2005).
[21] S. Pagola, P.W. Stephens, D.S. Bohle, A.D. Kosar, S.K. Madsen. *Nature*, **404**, 307 (2000).
[22] A. Dorn, R. Stoffel, H. Matile, A. Bubendorf, R.G. Ridley. *Nature*, **374**, 269 (1995).
[23] K. Waller, R. Muhle, L. Ursos, P. Horrocks, D. Verdier-Pinard, A. Sidhu, H. Fujioka, P. Roepe, D. Fidock. *J. Biol. Chem.*, **278**, 33593 (2003).
[24] M.A. Kadir, N. Mansor, M.S.M. Yusof, C.J. Sumby. *Complex Met.*, **1**, 32 (2014).

[25] J. Börner. Zinc complexes with N-donor ligands and their application as catalysts in the polymerisation of cyclic esters. Thesis, Universität Paderborn 2009.
[26] M. Darawsheh, H. Abu Ali, A.L. Abuhijleh, E. Rappocciolo, M. Akkawi, S. Jaber, S. Maloul, Y. Hussein. *Eur. J. Med. Chem.*, **82**, 152 (2014).
[27] P. Souza, L. Sanz, V. Fernández. *Z. Naturforsch*, **46b**, 767 (1991).
[28] H. Abu Ali, H. Fares, M. Darawsheh, E. Rappocciolo, M. Akkawi, S. Jaber. *Eur. J. Med. Chem.*, **89**, 67 (2015).
[29] V.K. Bel, A.I. Prisyazhnyuk, E.V. Kolchinskii, T.V. Koksharova. *J. Struct. Chem.*, **27**, 808 (1987).
[30] A.T. Hutton, D.A. Thornton. *Spectrochim. Acta, Part A*, **34**, 645 (1978).
[31] W.L. Steffen, G.J. Palenik. *Inorg. Chem.*, **16**, 1119 (1977).
[32] E. Deharo, P. Oporto, A. Gimenez, M. Sauvain, V. Jullian. *Exp. Parasitol*, **100**, 252 (2002).
[33] D.-76181 SMART-NT V5.6, Bruker AXS GMBH, Karlsruhe, Germany (2002).
[34] D.-76181 SAINT-NT V5.0, BRUKER AXS GMBH, Karlsruhe, Germany (2002).
[35] D.-76181 SHELXTL-NT V6.1, BRUKER AXS GMBH, Karlsruhe, Germany (2002).
[36] G. Blauer, M. Akkawi. *J. Inorg. Biochem.*, **66**, 145 (1997).